0026-895X/08/7404-941–951$20.00
MOLECULAR PHARMACOLOGY
Copyright © 2008 The American Society for Pharmacology and Experimental Therapeutics
Mol Pharmacol 74:941–951, 2008

Vol. 74, No. 4
48710/3383093
Printed in U.S.A.

Structural Determinants for Antagonist Pharmacology That Distinguish the ρ_1 $GABA_C$ Receptor from $GABA_A$ Receptors

Jianliang Zhang, Fenqin Xue, and Yongchang Chang

Division of Neurobiology, Barrow Neurological Institute, St. Joseph's Hospital and Medical Center, Phoenix, Arizona

Received May 6, 2008; accepted July 2, 2008

ABSTRACT

GABA receptor (GABAR) types C ($GABA_CR$) and A ($GABA_AR$) are both GABA-gated chloride channels that are distinguished by their distinct competitive antagonist properties. The structural mechanism underlying these distinct properties is not well understood. In this study, using previously identified binding residues as a guide, we made individual or combined mutations of nine binding residues in the ρ_1 $GABA_CR$ subunit to their counterparts in the $\alpha_1\beta_2\gamma_2$ $GABA_AR$ or reverse mutations in α_1 or β_2 subunits. The mutants were expressed in *Xenopus laevis* oocytes and tested for sensitivities of GABA-induced currents to the $GABA_A$ and $GABA_C$ receptor antagonists. The results revealed that bicuculline insensitivity of the ρ_1 $GABA_CR$ was mainly determined by Tyr106, Phe138 and Phe240 residues. Gabazine insensitivity of the ρ_1 $GABA_CR$ was highly dependent on Tyr102, Tyr106, and Phe138. The sensitivity of the ρ_1 $GABA_CR$ to 3-aminopropyl-phosphonic acid and its analog 3-aminopropyl-(methyl)phosphinic acid mainly depended on residues Tyr102, Val140, FYS240–242, and Phe138. Thus, the residues Tyr102, Tyr106, Phe138, and Phe240 in the ρ_1 $GABA_CR$ are major determinants for its antagonist properties distinct from those in the $GABA_AR$. In addition, Val140 in the $GABA_CR$ contributes to 3-APA binding. In conclusion, we have identified the key structural elements underlying distinct antagonist properties for the $GABA_CR$. The mechanistic insights were further extended and discussed in the context of antagonists docking to the homology models of $GABA_A$ or $GABA_C$ receptors.

The $GABA_A$ and $GABA_C$ receptors are both GABA-gated chloride channels but have distinct antagonist properties. The selective antagonism forms the basis for their classification. In fact, the $GABA_CR$ was defined as the GABA receptor that is insensitive to $GABA_A$ competitive antagonist bicuculline and $GABA_B$ receptor agonist baclofen (Drew et al., 1984; Johnston, 1996). In addition to bicuculline, $GABA_A$Rs can be antagonized by gabazine (SR95531). In contrast, $GABA_C$Rs are much less sensitive to gabazine but can be selectively antagonized by (1,2,5,6-tetrahydropyridine-4-yl)methylphosphinic acid (not available in the United States; Murata et al., 1996; Ragozzino et al., 1996), 3-aminopropyl(methyl) phosphinic acid (3-APMPA), and 3-aminopropylphosphonic acid (3-APA) (Johnston, 1996). Distinct antagonist profiles of the $GABA_A$ and $GABA_C$Rs indicate that their agonist/antagonist binding pockets are not the same. However, the structural basis for the distinct antagonist profiles of these two receptor types is not known.

Molecular cloning has identified at least 18 GABA receptor subunits in the nervous system (Barnard et al., 1998). They all belong to the cys-loop receptor family of the ligand-gated ion channels (Lester et al., 2004). A typical $GABA_AR$ can be formed by exogenously coexpressing α, β, and γ subunits with two α subunits, two β subunits, and one γ subunit in a receptor (Chang et al., 1996). The $\alpha_1\beta_2\gamma_2$ is the most abundant subtype of $GABA_A$Rs in the central nervous system (Whiting et al., 2000). The $GABA_C$Rs seemed to be mainly formed by ρ subunits (Zhang et al., 2001). When exogenously expressed, the ρ_1 GABA receptor subunit can form functional channels with the $GABA_CR$ pharmacological properties (Cutting et al., 1991).

Studies in the past 2 decades with photoaffinity labeling, site-directed mutagenesis, and the substituted cysteine accessibility method have shaped relatively complete models for the extracellular agonist/antagonist binding pockets of $\alpha\beta\gamma$ $GABA_AR$ (Sigel et al., 1992; Amin and Weiss, 1993; Smith and Olsen, 1994; Westh-Hansen et al., 1997, 1999; Boileau et al., 1999; Boileau et al., 2002; Holden and Czajkowski, 2003; Newell and Czajkowski, 2003) and the ρ_1 $GABA_CR$ (Amin and Weiss, 1994; Lummis et al., 2005; Sedelnikova et al., 2005; Harrison and Lummis, 2006). In the structural model of the $GABA_AR$, residues in six loops (segments) designated A through F have been identified to form

This work was supported by Arizona Biological Research Commission grant (ABRC0702) and by Barrow Neurological Foundation (to Y.C.).
Article, publication date, and citation information can be found at http://molpharm.aspetjournals.org.
doi:10.1124/mol.108.048710.

ABBREVIATIONS: $GABA_AR$, $GABA_A$ receptor; $GABA_CR$, $GABA_C$ receptor; 3-APA, 3-aminopropyl-phosphonic acid; 3-APMPA, 3-aminopropyl-(methyl)phosphinic acid.

the agonist/antagonist binding pocket in the subunit interface between β and α subunits. The β subunit contributes the binding loops A, B, and C. The α subunit contributes the binding loops D, E, and F. In contrast, the agonist/antagonist binding pocket of the ρ_1 $GABA_CR$ is formed in the subunit interface between two ρ_1 subunits with five binding loops (A–E) identified (Sedelnikova et al., 2005).

Figure 1 shows the aligned sequences of the binding loops in the $GABA_A$ and $GABA_C$ subunits. Note that the loop C of the ρ_1 subunit has one insertion (Ser242), which is close to an additional binding residue (Tyr241) in the same loop (Amin and Weiss, 1994). This alignment is further supported by our preliminary result that the receptor was not functional with three residues (Phe240–Ser242) of the ρ_1 subunit replaced by the corresponding residues in the β_2 subunit with previous alignment (data not shown). However, with a double mutation and a deletion (F240V+Tyr241F+S242Δ), the receptor was functional. For convenience, we refer to this F240V+Tyr241F+S242Δ mutant as a single mutant: FYS240VF. Other distinct binding residues in the $GABA_A$ and $GABA_CR$ subunits are apparent in the sequence alignment. Except for the residues in the extended loop E, which apparently do not face the binding pocket, the other nine distinct binding residues could potentially contribute to distinct antagonist pharmacology between $GABA_A$ and $GABA_C$Rs. These residues include Tyr102 and Tyr106 in loop D, Phe138 and Val140 in loop A, Ser168 in loop E, Tyr241 in loop C, and Leu216, Thr218 and Arg221 in loop F of the ρ_1 $GABA_CR$ subunit.

In this study, we substituted the distinct residues of the ρ_1 $GABA_CR$ subunit, indicated by arrowheads in Fig. 1, with the corresponding residues in the $GABA_AR$ β_2 (for loops A and C) or α_1 (for loops D, E, and F) subunits individually or in combinations. When these mutants were expressed in *Xenopus laevis* oocytes, they formed functional channels with altered sensitivities to agonists and antagonists. By testing antagonist sensitivity of agonist-induced current in these mutants, we have identified key structural elements underlying distinct antagonist properties for the $GABA_A$ and $GABA_C$Rs. The mechanistic insights for the selective interactions between the antagonists and two types of receptors were further discussed in the context of antagonist dockings to the homology models of the $GABA_A$ or $GABA_C$Rs.

Materials and Methods

Mutagenesis and cRNA Preparation. The cDNA encoding human ρ_1 GABA receptor subunit and rat α_1, β_2, and γ_2 GABA receptor subunits were kindly provided by Dr. David S. Weiss. Note that the rat GABA receptor subunits are highly homologous (98–99%) to their human counterparts. In fact, in all binding loops, these rat and human GABA receptor subunits are virtually identical. All subunits were cloned into the oocyte expression vector pGEMHE with T7 orientation. The residues in the amino-terminal segments corresponding to loops A, C, D, E, and F in the ρ_1 GABA receptor subunit were mutated to their homologous residues in the α_1 or β_2 GABA receptor subunits, individually or in combination, using the polymerase chain reaction-based QuikChange method of site-directed mutagenesis following the manufacturer's protocol (Stratagene, La Jolla, CA). The mutations were confirmed by automated DNA sequencing. The wild-type and mutant cDNAs were then linearized by NheI digestion. The cRNAs were transcribed with a standard in vitro transcription protocol as described previously (Sedelnikova et al., 2005). The cRNA yield and integrity were examined on a 1% agarose gel. cRNA concentration was further quantitated with an Eppendorf BioPhotometer (Eppendorf North America, New York, NY).

Oocyte Preparation and RNA Injection. Female *X. laevis* frogs (Xenopus I, Ann Arbor, MI) were anesthetized by 0.2% MS-222. The ovarian lobes were surgically removed from the frog and placed in the incubation solution, consisting of 82.5 mM NaCl, 2.5 mM KCl, 1 mM $MgCl_2$, 1 mM $CaCl_2$, 1 mM Na_2HPO_4, 0.6 mM theophylline, 2.5 mM sodium pyruvate, 5 mM HEPES, 50 μg/ml gentamicin, 50 U/ml penicillin, and 50 μg/ml streptomycin, pH 7.5. The frog was then given the analgesic xylazine hydrochloride (10 mg/kg i.p.) and allowed to recover from surgery in shallow water before being returned to the incubation tank. The lobes were cut into small pieces and digested with 1 Wünsch unit/ml Liberase Blendzyme 3 (Roche Applied Science, Indianapolis, IN) with constant stirring at room temperature for 1.5 to 2 h. The dispersed oocytes were thoroughly rinsed with the above solution. The stage VI oocytes were selected and incubated at 16°C before injection. Micropipettes for injection were pulled from borosilicate glass (Drummond Scientific, Broomall, PA) on a horizontal puller (P87; Sutter Instrument Company, Novato, CA), and the tips were cut with forceps to ≈40 μm in diameter. The cRNA was drawn up into the micropipette and injected into oocytes

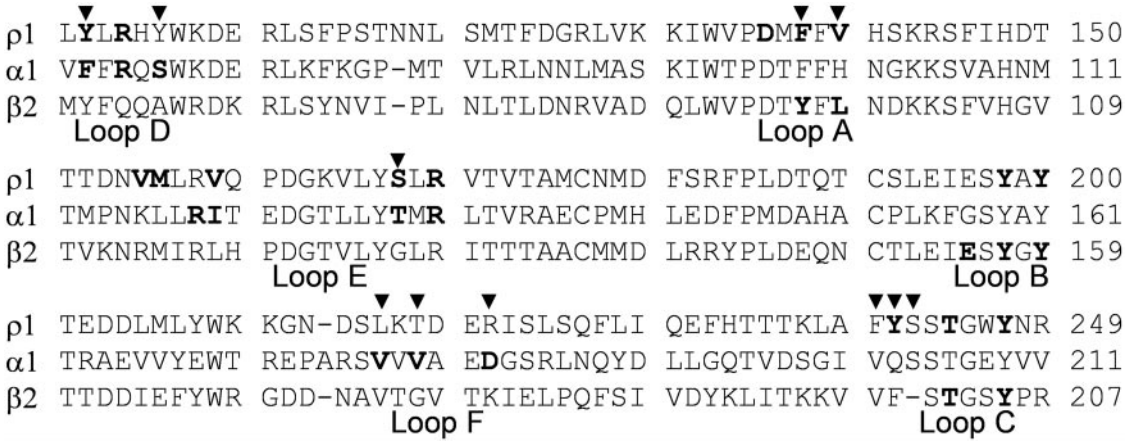

Fig. 1. Design of mutations based on the distinct binding residues in the $GABA_A$ and $GABA_C$Rs. Sequence alignment of the amino-terminal domains of the $GABA_A$ (α_1, β_2) and $GABA_C$ (ρ_1) receptor subunits with binding sites in bold. Except for an extended region of loop E (first three binding residues in loop E) that appears to not face the binding pocket in the structure model (Sedelnikova et al., 2005), all other distinct binding residues are potential binding residues underlying distinct antagonist pharmacological properties between the $GABA_A$ and $GABA_C$Rs. The residues pointed by arrowheads are the residues under investigation.

with a Nanoject microinjection system (Drummond Scientific) at a total volume of 20~60 nl.

Two-Electrode Voltage-Clamp. One to 3 days after injection, the oocyte was placed in a homemade small-volume chamber with continuous perfusion with oocyte Ringer's solution, which consisted of 92.5 mM NaCl, 2.5 mM KCl, 1 mM $CaCl_2$, 1 mM $MgCl_2$, and 5 mM HEPES, pH 7.5. The chamber was grounded through an agar bridge. The oocytes were voltage-clamped at −60 mV to measure GABA-induced currents using a GeneClamp 500B (Axon Instruments, Foster City, CA). The current signal was low-pass filtered at 10 Hz with the built-in low-pass Bessel filter in the GeneClamp 500B and digitized at 20 Hz with Axon Digidata1320 and pClamp9 (Molecular Devices, Sunnyvale, CA) in a Dell desktop computer. For the antagonist sensitivity test, GABA-induced current with an ~EC_{20} concentration, the concentration that induces 20% of maximum current, for each mutant was inhibited with coapplication of an antagonist with increasing concentrations. The antagonist IC_{50} (the concentration that inhibits 50% of GABA-induced current) was then determined by fitting concentration-dependent inhibition data with a Hill inhibition equation using Prism 4 software (GraphPad Software, San Diego, CA). The IC_{50} values were further used to calculate antagonist apparent affinity K_i for different mutants by the following equation: $K_i = IC_{50}/(1 + [GABA]/EC_{50})$ (Newell and Czajkowski, 2003).

Drug Preparation. GABA (SigmaAldrich, St. Louis, MO) stock solution (100 mM) was prepared daily from solid. (−)-Bicuculline methiodide (Tocris Bioscience, Ellisville, MO), gabazine (SR95531; Tocris), 3-APMPA (SKF97541; Tocris), and 3-APA (SigmaAldrich) stock solutions (20, 25, 100, and 100 mM, respectively) were prepared and stored at −20°C in aliquots before use.

Data Analysis. The dose-response relationship of the GABA-induced current in recombinant $GABA_{A/C}$ receptors was least-squares fit to a Hill equation with Prism 4.0 (GraphPad Software) to derive EC_{50}, Hill coefficient (the slope factor), and maximum current. The dose-dependent inhibition by competitive antagonists was fitted to a Hill inhibition equation to derive IC_{50}, Hill coefficient, and maximal current. The maximum current was then used to normalize the dose-response/-inhibition curve for each individual oocyte. The averages of the normalized currents were used to plot the data. All the data were presented as mean ± S.E.M. (standard error of the mean).

Homology Modeling. The three-dimensional model of the pentameric extracellular domains of the ρ_1 GABA receptor was made previously (Sedelnikova et al., 2005). The three-dimensional model of $\alpha_1\beta_2\gamma_2$ GABA receptor extracellular domain was built using Discovery Studio 1.7 software (Accelrys, San Diego, CA) running in a Dell Precision 690 computer (Dell, Austin, TX) with the homology model of the ρ_1 GABA receptor as the template to ensure that two homology models converge in a similar way for better comparison. In brief, amino-terminal domains of the rat GABA receptor subunits ($\beta_2\alpha_1\beta_2\alpha_1\gamma_2$) were aligned to the human ρ_1 sequences (chains A to E) with the modeler in the Discovery Studio Modeler 9 using "Align Sequence with Structure" protocol (Sali and Blundell, 1993) with blosum62 scoring matrix, gap open penalty of −100, gap extension penalty of −10, and default two-dimensional gap weights. The homology models were then built using "Building Homology Models" (Sali and Blundell, 1993). The pentameric model was further energy minimized for 400 steps of the "Steepest Descent" minimization followed by 1000 steps of "Conjugated Gradient" minimization using "Minimization" protocol with CHARMm force field. The model of mutant receptor with mutation(s) in the binding regions was generated with "Build Mutant" protocol and energy minimized as above.

Ligand Docking. The three-dimensional ligand structures of bicuculline, gabazine, 3-APA, and 3-APMPA were downloaded, as MDL molecule files, from the ChemIDplus National Institutes of Health web site (http://chem.sis.nlm.nih.gov/chemidplus/). The receptor subunit dimers were saved from original pentameric models. The docking of flexible ligands to the putative binding pockets of the $GABA_A$ (in the interface between β_2 and α_1 subunits) or $GABA_C$ (in the interface between two ρ_1 subunits) receptors was performed with "Dock Ligands (LigandFit)" protocol (Venkatachalam et al., 2003) in the Discovery Studio 1.7 software (Accelrys, San Diego, CA). The docking results were scored with all available scoring functions, which include DockScore [= −(ligand/receptor interaction energy + ligand internal energy)], LigScore1 and LigScore2 (Krammer et al., 2005), Ludi1 (Böhm, 1994) and Ludi2 (Böhm, 1998), Piecewise Linear Potential 1 (Gehlhaar et al., 1995) and Piecewise Linear Potential 2 (Gehlhaar et al., 1999), potential of mean force (Muegge and Martin, 1999), and Jain (Jain, 1996). The poses with the highest DockScores tended to have highest scores in other functions, although the scores from these scoring functions in different poses were only partially correlated (data not shown). Thus, the poses with highest DockScores and the lowest ligand internal energy were used for presentation unless specified otherwise. The docking success [with output pose(s)] was determined by pose saving thresholds. We used default values of Pose Saving Dockscore Threshold (0.0), Pose Saving RMS Threshold for Diversity (1.50), and Pose Saving Score Threshold for Diversity (20.0). A docking without any output pose is considered as a failure.

Results

Bicuculline Sensitivity. Bicuculline insensitivity is the major distinction of $GABA_CRs$ from $GABA_ARs$. To search for the structural basis underlying this difference, we first made individual mutations, except for Tyr241 (FYS240VF), in nine distinct binding site residues in the ρ_1 $GABA_CR$ to their counterparts in the α_1 or β_2 $GABA_AR$ subunits. When expressed in *X. laevis* oocytes, all nine individual mutant ρ_1 GABA receptors resulted in functional channels with slightly altered GABA sensitivity (with maximum of 24-fold reduction). The EC_{50} values and maximal currents (I_{max}s) derived from GABA dose-response relationships of these mutants are listed in Table 1. The GABA-induced current with an ~EC_{20} GABA concentration was then used to test bicuculline sensitivity of these mutants. Figure 2A represents the dose-dependent inhibition of the GABA-induced currents by bicuculline in the wild-type and single mutant ρ_1 GABA receptors. Note that although the wild-type ρ_1 $GABA_CR$ was essentially insensitive to bicuculline, three (of nine) mutants (Y106S, F138Y and FYS240VF) exhibited slightly increased sensitivity to bicuculline (Fig. 2A). At the highest concentrations tested, bicuculline blocked nearly one half of the GABA-induced currents in these three mutants. Due to incomplete inhibition (<50%) at the highest concentrations tested, the IC_{50} values could not be reliably determined. They were clearly slightly higher than the highest concentrations tested in these three mutants. The range of IC_{50} values and derived apparent affinity K_i are listed in Table 2. The result suggests that these three mutants are potential candidates for further investigation.

By making single mutations at these nine distinct binding residues in the ρ_1 $GABA_CR$ subunit, we were clearly unable to dramatically increase binding affinity to bicuculline. However, we could potentially achieve this goal by combining several promising individual mutants. To test this, we made double and triple mutants with combinations of the three promising individual mutants. Figure 2B represents bicuculline dose-inhibition for the combinations of these promising mutants along with one nonpromising mutant as a control. Double mutations (Y106S+FYS240VF, Y106S+F138Y, F138Y+FYS240VF) clearly in-

creased bicuculline sensitivity of the receptor. The triple mutant Y106S+F138Y+FYS240VF exhibited the highest bicuculline sensitivity (K_i = 28.85 ± 1.96 μM, Table 2), which was only severalfold lower than the bicuculline sensitivity of the wild-type $GABA_AR$ (K_i = 5.21 ± 0.74 μM, Table 2). Thus, mutations of these residues to their homologous residues in the $GABA_AR$ are enough to confer bicuculline sensitivity to the ρ_1 $GABA_CR$. These residues must synergistically contribute to bicuculline affinity, although we cannot role out the contribution of other binding and "nonbinding" residues to bicuculline binding. For individual contributions of the residues Phe240 and Tyr241 in FYS240VF mutant, please see *Discussion*.

Gabazine Sensitivity. Like bicuculline, gabazine is also a relatively selective $GABA_AR$ antagonist, although their structures are quite different. In fact, gabazine has a nanomolar affinity for $GABA_AR$. However, the wild-type ρ_1 $GABA_CR$ was still sensitive to gabazine but with a much lower affinity (K_i = 57.84 ± 7.66 μM) compared with K_i = 0.12 ± 0.01 μM in the wild type $GABA_AR$ (Table 3). Figure 3A represents gabazine dose-inhibition relationships in nine individual mutants of the ρ_1 GABA receptor. Note that whereas FYS240VF mutation increased apparent affinity by only ~2-fold, the other three mutants (Y102F, Y106S, and F138Y) exhibited a larger increase in gabazine affinity (with decreased K_i; Table 3). Combination of Y102F, Y106S, and F138Y resulted in a receptor with a much lower K_i (1.61 ± 0.03 μM) despite a dramatic increase in GABA EC_{50} (156.46 ± 10.73 μM) for this mutant receptor. Thus, residues Tyr102, Tyr106, and Phe138 are major contributors to gabazine binding. Other minor contributors include Ser168 and Thr218. Mutations of them increased gabazine affinity by approximately 5-fold.

3-APA and 3-APMPA Sensitivity. 3-APA and its methylated analog 3-APMPA are selective competitive antagonists for $GABA_C$ over $GABA_ARs$ (Johnston, 1996), although they are also $GABA_B$ receptor agonists (Froestl et al., 1995). Mutants Y102F, V140L, and FYS240VF exhibited the most dramatic reduction of apparent affinity to the $GABA_CR$ competitive antagonist 3-APA (11-, 32-, and 25-fold reduction, respectively, Fig. 4A and Table 4). Thus, bicuculline and 3-APA both interact with three binding loops (D, A, and C) but with slightly different residues in loops D and A. We predicted that when all three residues are mutated, the sensitivity to 3-APA should be further reduced. Indeed, the triple mutant Y102F+Val140L+FYS240VF exhibited 77-fold reduction in sensitivity to 3-APA (Fig. 4B and Table 4).

Because the triple mutant is still slightly sensitive to 3-APA (K_i = 844.88 ± 100.67 μM), we then combined two additional mutations (Y106S and F138Y) to the receptor. When the quintuple mutant was expressed, it exhibited bicuculline sensitivity (although reduced compared with the triple mutant; Table 2) and 3-APA insensitivity (Fig. 4C). Further reduction of 3-APA sensitivity in the quintuple mutant could be due to the contribution of F138Y mutation, which reduced 3-APA sensitivity by 7.5-fold when singly mutated. Thus, we have identified five residues in the binding site that conferred $GABA_C$ properties to the ρ_1 GABA receptor, and

TABLE 1

EC_{50} and I_{max} values of the GABA-induced currents for all mutants

Note that although we injected similar amount of RNA for all constructs, the expression levels were not strictly controlled because of batch-to-batch variability of oocytes and testing date after injection. Thus, I_{max} cannot be used to estimate the influence of gating on EC_{50}. Because most mutants have the I_{max} values that were not dramatically reduced, the contribution of gating influence on EC_{50} are relatively small in these mutants. However, we noted that Y106S+F138Y+V140L+FYS240VF and Y102F+Y106S+F138Y+V140L+FYS240VF ρ1 mutants have relatively low expression. This is further confirmed by comparison of their expression levels to the wild-type receptor in the same batch of oocytes and in the same time period after injection. The results showed that the I_{max} values for Y106S+F138Y+V140L+FYS240VF and Y102F+Y106S+F138Y+V140L+FYS240VF were 13 and 15% of the wild type expression level respectively.

	Mutants	*n*	EC_{50}	I_{max}
			μM	*nA*
$GABA_CR$ (ρ1)	WT	3	0.88 ± 0.02	1017 ± 97
	Y102F	4	0.67 ± 0.04	1626 ± 325
	Y106S	3	4.94 ± 0.30	1823 ± 141
	F138Y	3	20.43 ± 0.21	3862 ± 423
	V140L	4	21.18 ± 1.80	1439 ± 43
	S168T	4	10.91 ± 0.42	2104 ± 293
	L216V	3	0.16 ± 0.00	3414 ± 380
	T218V	4	1.01 ± 0.01	3048 ± 117
	R221D	4	0.26 ± 0.01	3200 ± 225
	FYS240VF	3	20.54 ± 0.49	3192 ± 679
	Y106S+F138Y	3	93.51 ± 2.90	2373 ± 94
	Y106S+FYS240VF	4	49.29 ± 3.16	513 ± 64
	F138Y+FYS240VF	4	1.62 ± 0.07	3415 ± 149
	Y106S+F138Y+FYS240VF	3	2.58 ± 0.09	3544 ± 538
	Y102F+Y106S+F138Y	5	156.46 ± 10.73	1098 ± 143
	Y102F+F138Y+FYS240VF	4	10.00 ± 0.65	2424 ± 219
	Y102F+V140L+FYS240VF	4	229.63 ± 12.73	1217 ± 155
	Y106S+F138Y+V140L+FYS240VF	4	76.03 ± 3.13	254 ± 4
	Y102F+Y106S+F138Y+V140L+FYS240VF	4	87.34 ± 5.26	221 ± 31
$GABA_AR$ ($\alpha1\beta2\gamma2$)	$\alpha1\beta2\gamma2$_WT	3	21.24 ± 2.82	2873 ± 279
	$\alpha1$(S68Y)$\beta2\gamma2$	3	3.78 ± 0.16	3425 ± 112
	$\alpha1$(V178L)$\beta2\gamma2$	3	1.79 ± 0.41	2933 ± 163
	$\alpha1$(D183R)$\beta2\gamma2$	4	0.89 ± 0.09	3415 ± 409
	$\alpha1\beta2$(Y97F)$\gamma2$	3	3.81 ± 0.36	4959 ± 409
	$\alpha1\beta2$(VF199FYS)$\gamma2$	3	55.48 ± 12.24	5156 ± 308
	$\alpha1$(S68Y)$\beta2$(Y97F)$\gamma2$	3	13.35 ± 0.56	5947 ± 86
	$\alpha1$(S68Y)$\beta2$(VF199FYS)$\gamma2$	3	39.59 ± 9.03	2246 ± 89
	$\alpha1$(S68Y)$\beta2$(Y97F+VF199FYS)$\gamma2$	3	41.61 ± 6.52	3483 ± 446
	$\alpha1$(F64Y+S68Y)$\beta2$(Y97F+L99V+VF199FYS)$\gamma2$	4	15.58 ± 1.65	3391 ± 91

the combined mutation of these residues converted the ρ_1 GABA receptor to the GABA$_A$R antagonist pharmacology.

3-APMPA has a structure similar to that of 3-APA. Using high concentrations of 3-APMPA to test all mutants is cost-prohibitive. Thus, we tested only its sensitivity in the quintuple mutant. Indeed, the quintuple mutant also exhibited insensitivity to 3-APMPA. At the concentration of 1500 μM, 3-APMPA only inhibited the GABA-induced current by approximately 30% (data not shown). Thus, residues Tyr102, Phe138, Val140, and potentially Tyr241 are important determinant for 3-APA and 3-APMPA binding.

Corresponding Mutants in GABA$_A$R Partially Converted the Receptor to GABA$_C$ Pharmacology. If the identified residues in GABA$_C$R are major determinants for its antagonist specificity, we should expect that mutations of these residues in GABA$_A$R also convert its pharmacological properties to GABA$_C$R. In the GABA$_A$R, loops A and C are in the β subunit, whereas loop D is in the α subunit. The three mutants corresponding to the Y106S, F138Y, and FYS240VF in the ρ_1 GABA$_C$R for bicuculline sensitivity are α_1(S68Y), β_2(Y97F), and β_2(VF199FYS). In fact, single mutations of α_1(S68Y) or β_2(Y97F) reduced the receptor sensitivity to bicuculline (Table 2 and Fig. 5A). Thus, α_1 Ser68 and β_2 Tyr97 are important determinants of GABA$_A$R bicuculline sensitivity. In contrast, the mutant β_2VF199FYS in the loop C slightly increased bicuculline sensitivity (Table 2). This opposite effect will be discussed in more detail under *Discussion*. When the quintuple mutant (triple mutant β_2 subunit coexpressed with the double mutant α_1 subunit) in the GABA$_A$R, corresponding to the quintuple mutant of the GABA$_C$R in Fig. 4, C and D, the receptor exhibited a significant reduction in bicuculline (Table 2) and gabazine (Fig. 5B) sensitivity and became slightly sensitive to 3-APA (data not shown). The results further support the importance of these five binding residues for the GABA$_A$ and GABA$_C$R antagonist properties.

Discussion

In search of the structural basis of the distinct antagonist properties of GABA$_A$ and GABA$_C$Rs, we have identified several key binding residues in loops D, A, and C as major determinants for GABA$_C$R antagonist specificity. The results revealed that bicuculline sensitivity was mainly conferred by

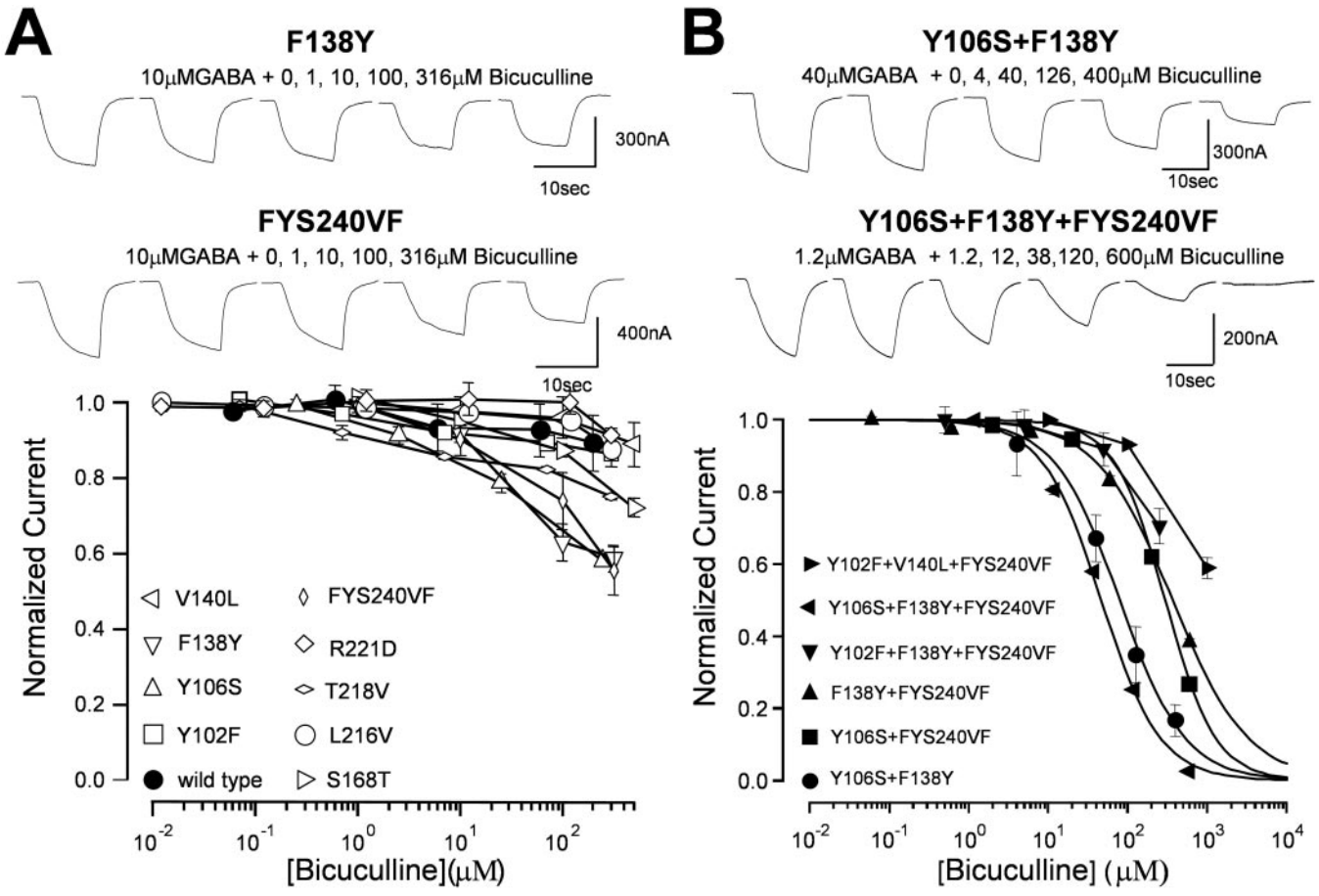

Fig. 2. Effect of nine individual mutations and their combinations of the ρ_1 GABA$_C$R on the sensitivity to bicuculline. A, effect of individual mutations. Top, examples of GABA (~EC$_{20}$)-induced current traces blocked by increasing concentrations of bicuculline. Bottom, normalized and averaged bicuculline dose-inhibition of the wild type and nine mutant receptors ($n \geq 3$ for each construct). Note that at the highest concentration, bicuculline blocked only <10% of the GABA-induced current in the wild-type receptor. In contrast, bicuculline blocked >40% of the GABA-induced currents in three mutants (Y106S, F138Y, and FYS240VF). Because the maximal inhibitions were less than 50%, dose-inhibition fitting could not generate reliable results and was not performed. Instead, straight lines are used to link the points for each construct (WT or mutant). B, effect of double and triple mutations on bicuculline sensitivity ($n \geq 3$ for each construct). Top, examples of GABA(~EC$_{20}$)-induced current traces blocked by increasing concentrations of bicuculline. Bottom, normalized and averaged bicuculline dose-inhibition of the double or triple mutants. Continuous lines are best fits of the data to a Hill inhibition equation, and the resulting IC$_{50}$ values are listed in Table 2. Note that the triple mutant containing Y106S, F138Y, and FYS240VF exhibited highest sensitivity to bicuculline.

the mutations Y106S, F138Y, and FYS240VF. Gabazine sensitivity was highly dependent on the mutations Y106S, F138Y, and Y102F. For the $GABA_CR$ antagonist 3-APA, its sensitivity was mainly dependent on residues Tyr102, Val140, FYS240–242, and Phe138. Thus, the residues Tyr102, Tyr106, Phe138, and FYS240–242 in the ρ_1 $GABA_CR$ are major determinants for the $GABA_CR$ antagonist properties distinct from those in the $GABA_AR$. In addition, Val140 in the $GABA_CR$ also contributes to the 3-APA binding. To gain further insights from our findings, we performed homology modeling and ligand docking for both $GABA_A$ and $GABA_CRs$ and provided further experimental evidence to dissect individual contribution of FYS240–242.

Bicuculline Sensitivity. We have successfully docked bicuculline into the putative $GABA_AR$ binding pocket but failed in docking bicuculline into the $GABA_CR$ binding pocket. Figure 6A shows the docked bicuculline in the $GABA_AR$ binding pocket. Note that three putative hydrogen bonds are formed between the docked bicuculline molecule and residues β_2 Tyr97 (loop A), β_2 Tyr157 (loop B), or α_1 Arg66 (loop D). Interaction of bicuculline to β_2 Tyr97 is supported by that a single β_2 Y97F mutation dramatically reduced the $GABA_AR$ sensitivity to bicuculline (Table 2, Fig. 5A). The homologous residue in the $GABA_CR$ is ρ_1 Phe138. However, the F138Y mutation only slightly increased the $GABA_CR$ affinity to bicuculline, presumably by forming a hydrogen bond with bicuculline. Thus, other residues must make substantial contributions to the bicuculline insensitivity of $GABA_CR$. β_2 Tyr157 and α_1 Arg66 of $GABA_AR$ are binding residues (Amin and Weiss, 1993; Harrison and Lummis, 2006). They are the same as their homologs ρ_1 Tyr198 and ρ_1 Arg104 in the

TABLE 2
IC_{50} and K_i values of $GABA_AR$ competitive antagonist, bicuculline, on GABA-induced current for all mutants.

	Mutants	IC_{50}	K_i	n
		μM		
$GABA_CR$ (ρ_1)	WT	>>>200	>>>119	3
	Y102F	>>>300	>>>146	4
	Y106S	>250	>166	4
	F138Y	>306	>212	4
	V140L	>>>500	>>>339	4
	S168T	>>500	>>260	4
	L216V	>>>300	>>>171	3
	T218V	>>300	>>177	4
	R221D	>>>300	>>>205	3
	FYS240VF	>316	>213	4
	Y106S+F138Y	72.18 ± 13.68	50.56 ± 9.58	3
	Y106S+FYS240VF	295.78 ± 7.81	154.62 ± 4.08	4
	F138Y+FYS240VF	366.70 ± 16.72	267.59 ± 12.20	4
	Y106S+F138Y+FYS240VF	42.27 ± 2.86	28.85 ± 1.96	6
	Y102F+F138Y+FYS240VF	>>250	>>166	4
	Y102F+V140L+FYS240VF	>1000	>695	3
	Y106S+F138Y+V140L+FYS240VF	251.53 ± 40.52	164.82 ± 26.55	4
	Y102F+Y106S+F138Y+V140L+FYS240VF	1052.55 ± 160.09	584.27 ± 88.87	4
$GABA_AR$	$\alpha1\beta2\gamma2$_WT	7.17 ± 1.01	5.21 ± 0.74	4
	$\alpha1$(S68Y)$\beta2\gamma2$	15.97 ± 1.01	12.12 ± 0.76	3
	$\alpha1\beta2$(Y97F)$\gamma2$	>>120	>>91	3
	$\alpha1\beta2$(VF199FYS)$\gamma2$	2.59 ± 0.12	1.68 ± 0.08	4
	$\alpha1$(S68Y)$\beta2$(Y97F)$\gamma2$	>>>120	>>>68.54	3
	$\alpha1$(S68Y)$\beta2$(VF199FYS)$\gamma2$	12.65 ± 0.35	10.10 ± 0.28	4
	$\alpha1$(S68Y)$\beta2$(Y97F+VF199FYS)$\gamma2$	>>100	>>81	4
	$\alpha1$(F64Y+S68Y)$\beta2$(Y97F+L99V+VF199FYS)$\gamma2$	100.01 ± 6.37	75.71 ± 4.81	4

>>>, inhibition was less than 20% at the concentration indicated; >>, inhibition was 20 to 40% at the concentration indicated; >, inhibition was between 40 and 50% at the concentration indicated.

TABLE 3
IC_{50} and K_i values of the $GABA_AR$ competitive antagonist, gabazine, on GABA-induced current for all mutants.

	Mutants	IC_{50}	K_i	n
		μM		
$GABA_CR$ (ρ_1)	WT	97.29 ± 11.52	57.84 ± 7.66	5
	Y102F	5.77 ± 1.01	3.98 ± 0.69	3
	Y106S	3.04 ± 0.27	2.13 ± 0.21	4
	F138Y	14.04 ± 1.74	9.74 ± 1.21	4
	V140L	322.85 ± 12.84	206.09 ± 8.20	4
	S168T	19.86 ± 2.02	13.62 ± 1.39	4
	L216V	326.72 ± 29.44	186.70 ± 16.83	3
	T218V	20.68 ± 3.94	11.54 ± 2.20	4
	R221D	53.37 ± 2.51	27.21 ± 1.28	4
	FYS240VF	39.07 ± 4.66	27.16 ± 3.24	4
	Y106S+F138Y	2.56 ± 0.18	1.73 ± 0.12	4
	Y106S+FYS240VF	5.80 ± 0.49	4.12 ± 0.31	4
	F138Y+FYS240VF	16.68 ± 0.51	12.16 ± 0.37	3
	Y102F+Y106S+F138Y	2.64 ± 0.05	1.61 ± 0.03	3
	Y106S+F138Y+FYS240VF	2.69 ± 0.24	1.83 ± 0.16	3
$GABA_AR$	$\alpha1\beta2\gamma2$_WT	0.15 ± 0.01	0.12 ± 0.01	3
	$\alpha1$(F64Y+S68Y)$\beta2$(Y97F+L99V+VF199FYS)$\gamma2$	3.54 ± 0.35	2.67 ± 0.26	4

$GABA_CR$ and thus do not contribute distinct bicuculline sensitivity.

To further dissect contributions of individual residues in the FYS240FY mutant in loop C, we first examined the homology model of $GABA_CR$. The loop C of the $GABA_CR$ has two aromatic residues, Phe240 and Tyr241 (a binding residue). The corresponding region in $GABA_AR$ has only one phenylalanine aligned to Tyr241. In addition, the position of these two aromatic residues could be altered by one insertion, Ser242. In the model, both residues (Phe240 and Tyr241) are lining the binding pocket. Because bicuculline is a large molecule, it is possible that this additional aromatic residue, Phe240, provides a steric hindrance for bicuculline binding. In fact, virtual F240V mutation in the $GABA_CR$ homology model increased the size of the binding pocket. Consequently, we were able to dock the bicuculline into the binding pocket of this mutant $GABA_CR$ model (data not shown). This effect was confirmed experimentally; whereas GABA sensitivity of the ρ_1 F240V mutant was similar to that of the wild type (but with a substantially reduced efficacy), this mutant did exhibit bicuculline sensitivity (K_i = 67.4 ± 0.5 μM). This further supports the notion that Phe240 in $GABA_C$ provides steric hindrance for bicuculline binding. In contrast, Y241F mutant remained insensitive to bicuculline (data not shown), suggesting that ρ_1 Tyr241 does not contribute to bicuculline insensitivity. Note that the reverse mutation in the $GABA_AR$ (β_2VF199FYS) did not reduce bicuculline sensitivity. In the $GABA_CR$ binding pocket, a residue near the Phe240 is the Asp219 in loop F. This negatively charged residue may provide electrostatic repulsion to the bicuculline, because the homologous residue in $GABA_AR$ is α_1 Ala181, a small and noncharged residue. Thus, it may need both Phe240 and Asp219 acting collaboratively to narrow the bottom of the binding pocket, preventing bicuculline binding.

As for Tyr106 in loop D, ρ_1 Y106S mutation improved sensitivity to bicuculline. The reverse mutation in the $GABA_AR$ (α_1 S68Y) reduced bicuculline sensitivity (Table 2). ρ_1 Tyr106 is next to Arg104, which is equivalent to α_1 R66 (making hydrogen bonding to bicuculline). It is possible that steric hindrance of loop C in the $GABA_CR$ pushes bicuculline

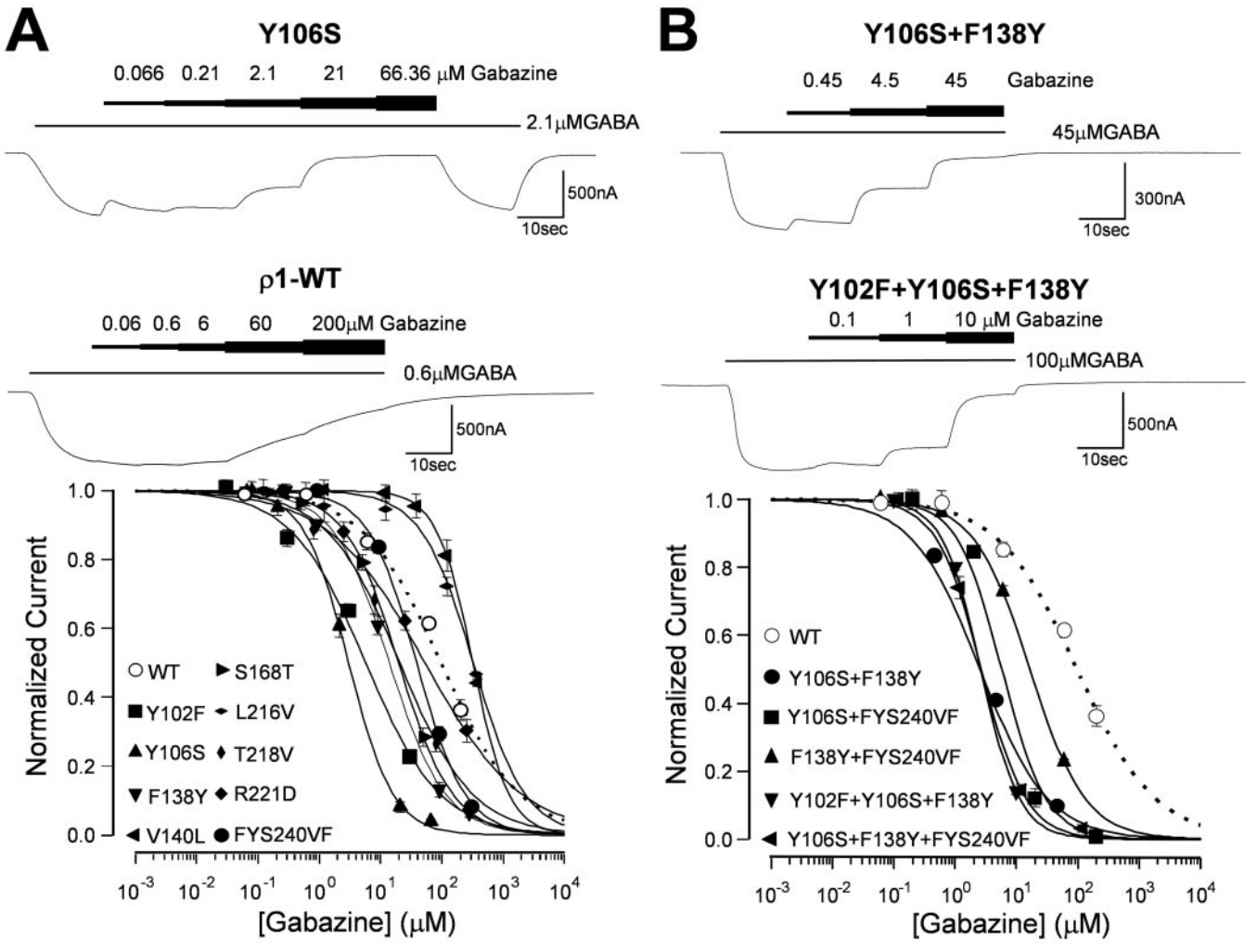

Fig. 3. Effect of nine individual mutations and their combinations of the ρ_1 $GABA_CR$ on the sensitivity to gabazine. A, effect of individual mutations. Top, examples of GABA (EC_{20})-induced current traces blocked by increasing concentrations of gabazine. Bottom, normalized and averaged gabazine dose-inhibition of the wild-type and nine mutant receptors ($n \geq 3$ for each construct). The continuous lines are best fits of the data to a Hill inhibition equation, and the resulting IC_{50} values are listed in Table 3. B, effect of double and triple mutations on gabazine sensitivity ($n \geq 3$ for each construct). Top, examples of GABA (~EC_{20})-induced current traces blocked by increasing concentrations of gabazine. Bottom, normalized and averaged gabazine dose inhibition of the GABA-induced currents in the double or triple mutants. The continuous lines are best fits of the data to a Hill inhibition equation. The dashed line is the fit of gabazine inhibition of the GABA-induced current in the wild type receptor.

to an upper position (Y106S), shifting hydrogen bonding from Arg104 to Y106S. The bulky Tyr106 may protrude too far so that it cannot form a hydrogen bond to bicuculline. However, when it was mutated to serine, the distance to bicuculline became closer.

Influence of Other Nearby Residues Although addition of Y102F and Val140L mutations to the triple mutant further decreased 3-APA sensitivity, it also unexpectedly resulted in a decrease in bicuculline sensitivity. This reduction could partially due to gating effect because the quadruple and quintuple

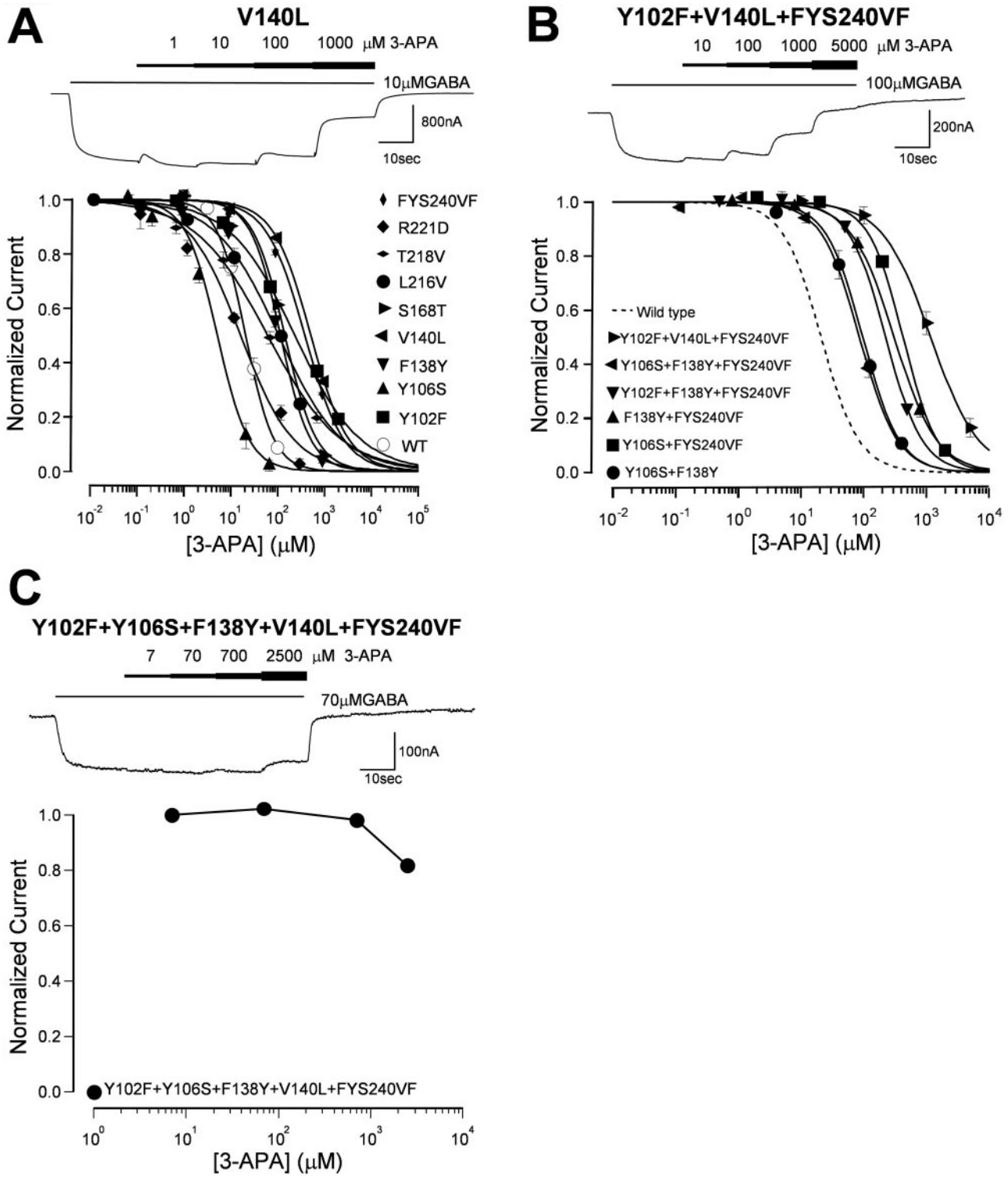

Fig. 4. Effect of mutations of the ρ_1 $GABA_CR$ on the sensitivity to 3-APA. A, effect of individual mutations on 3-APA inhibition of the receptor. Top, an example of GABA-induced current traces blocked by increasing concentrations of 3-APA. Bottom, normalized and averaged 3-APA dose-inhibition of the wild type and nine single mutant receptors. The continuous lines are best fits of the data to a Hill inhibition equation, and the resulting IC_{50} values are listed in Table 4. B, effect of double and triple mutations on 3-APA sensitivity. The continuous lines are best fits of the data to a Hill inhibition equation, and the resulting IC_{50} values are listed in Table 4. C, effect of quintuple mutations on 3-APA sensitivity. Because of limited inhibition, fitting was not performed. Straight lines are used to link multiple points.

mutants exhibited significantly reduced maximal current (Table 1). We re-tested I_{max} values in the quadruple and quintuple mutants and compared them with the wild type (Table 1 legend). Both mutants exhibited approximately a 7-fold reduction of I_{max}. Three-binding-to-open model (Amin and Weiss, 1996; Chang et al., 2000) predicts that EC_{50} shift due to this I_{max} reduction could account for ~2.7-fold increase in EC_{50} value. Thus, the calculated K_i could be underestimated by ~2-fold as a result of reduction of gating efficiency. In addition, trivial contributions of many other nearby nonbinding residues may influence the conformation in the binding site, making the GABA$_A$R more sensitive to bicuculline.

Gabazine Sensitivity. Our results suggest that Tyr102, Tyr106, and Phe138 are important residues that make the

TABLE 4
IC_{50} and K_i values of the GABA$_C$R competitive antagonist, 3-APA, on GABA-induced current for all mutants.

	Mutants	IC_{50}	K_i	n
		μM		
GABA$_C$R (ρ_1)	WT	21.03 ± 1.79	11.02 ± 0.94	3
	Y102F	237.86 ± 26.42	116.33 ± 12.92	4
	Y106S	5.43 ± 0.75	3.81 ± 0.59	4
	F138Y	118.57 ± 9.10	82.31 ± 6.32	4
	V140L	523.06 ± 11.33	355.31 ± 7.69	4
	S168T	144.67 ± 7.20	75.48 ± 3.75	4
	L216V	106.70 ± 9.30	60.97 ± 5.31	3
	T218V	61.67 ± 5.28	36.42 ± 3.12	4
	R221D	16.42 ± 1.63	11.24 ± 1.11	3
	FYS240VF	391.52 ± 11.11	272.24 ± 7.73	4
	Y106S+F138Y	96.61 ± 8.71	67.67 ± 6.10	3
	Y106S+FYS240VF	429.03 ± 14.41	305.20 ± 10.25	4
	F138Y+FYS240VF	309.79 ± 36.77	207.37 ± 24.61	3
	Y106S+F138Y+FYS240VF	87.22 ± 7.16	59.53 ± 4.88	3
	Y102F+F138Y+FYS240VF	226.87 ± 3.47	151.24 ± 2.31	3
	Y102F+V140L+FYS240VF	1212.82 ± 144.50	844.88 ± 100.67	4
	Y106S+F138Y+V140L+FYS240VF	>2500	>1299.64	4
	Y102F+Y106S+F138Y+V140L+FYS240VF	>>2500	>>1374.82	4

>>, inhibition was 20 to 40% at the concentration indicated; >, inhibition was between 40 to 50% at the concentration indicated.

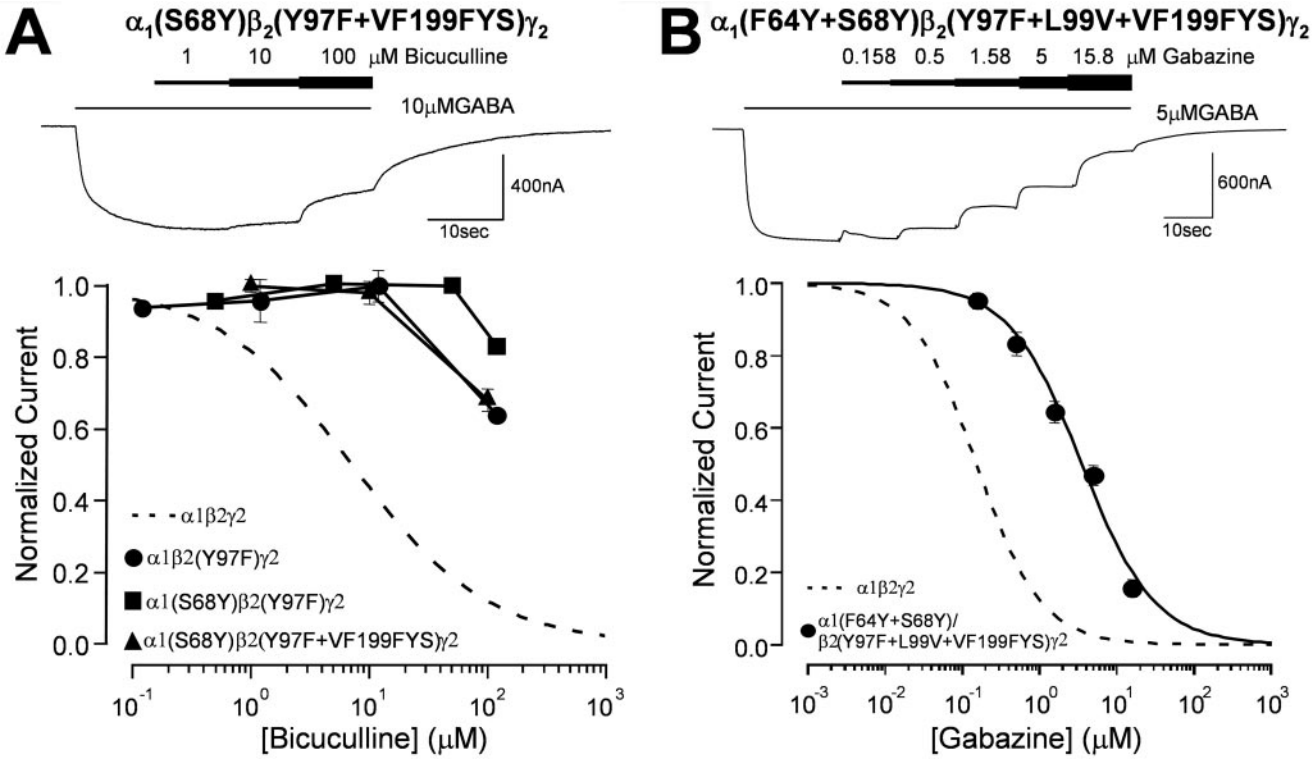

Fig. 5. Mutations of the GABA$_A$R in the corresponding residues partially converted the receptor to GABA$_C$ antagonist properties. A, effect of mutations of the GABA$_A$R on bicuculline sensitivity. The GABA receptor β_2Y97F mutation resulted in more than 10-fold decrease in bicuculline sensitivity. Coexpression of this mutant with the α_1S68Y mutant resulted in further reduction in bicuculline sensitivity. This further reduction of bicuculline sensitivity was counteracted by adding the third mutation β_2VF199FYS to the receptor. The dashed line represents the normalized dose-inhibition of GABA-induced current by bicuculline in the wild-type GABA$_A$R. B, the quintuple mutant of the GABA$_A$R to their homologous residues in the ρ_1 GABA$_C$R reduced gabazine sensitivity. Top, an example of a GABA-induced current inhibited by increasing concentrations of gabazine. Bottom, normalized and averaged dose-inhibition of the GABA-induced current by gabazine. Continuous line is the best fit of the data to a Hill inhibition equation. The resulting IC_{50} is listed in Table 3. Dashed line represents the normalized dose-inhibition of GABA-induced current by gabazine in the wild type GABA$_A$R.

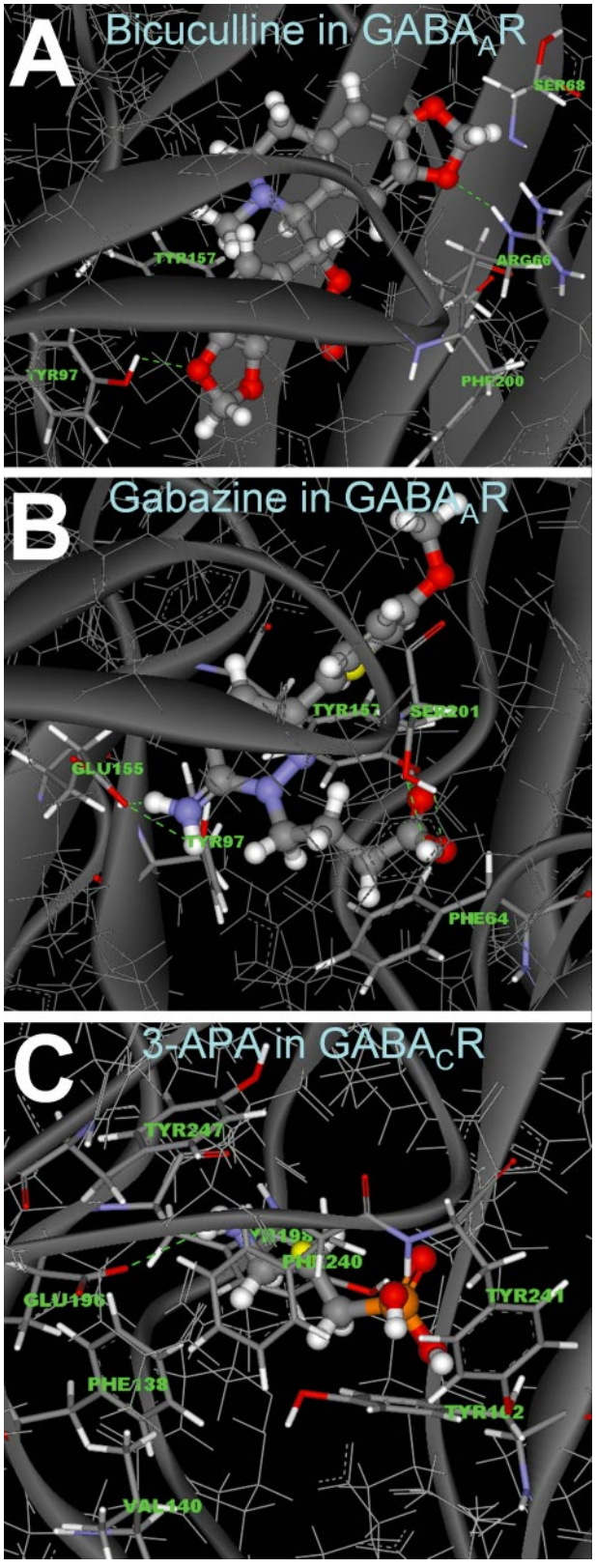

Fig. 6. Structural models of the $GABA_A$ or $GABA_C$R amino-terminal domains docked with antagonists. A, bicuculline docked to the $GABA_A$R binding pocket. Note that the docked bicuculline formed hydrogen bonds with three residues in loops A (β_2 Tyr97), D (α_1 Arg66), and B (β_2 Tyr157) (not visible in this view), and was also in close vicinity to α_1 Ser68. B, gabazine docked to the $GABA_A$R binding pocket. Note that the docked gabazine molecule formed hydrogen bonding with four residues in loops A (β_2Y97), B (β_2 Glu155 and β_2 Tyr157), and C (β_2 Ser201). C, 3-APA docked to $GABA_C$R binding pocket. The docked 3-APA molecule can form a hydrogen bond with Glu196 in loop B of the ρ_1 GABA receptor subunit, homologous to β_2 Glu155 in the $GABA_A$R. Note that the docked 3-APA resided in the aromatic box formed by Phe138, Phe240, Tyr241, and Tyr102 [and Tyr247 and Tyr198 (behind)].

$GABA_C$R less sensitive to gabazine, and FYS240VF is not important for gabazine sensitivity. The result is consistent with a previous finding in the $GABA_A$R: α_1 F64 (homologous to ρ_1 Tyr102) and β_2 Tyr97 (homologous to ρ_1 Phe138) are binding residues for gabazine (Boileau et al., 2002; Holden and Czajkowski, 2002). To get structural insights into the mechanism, we successfully docked gabazine molecule into the binding pockets of both $GABA_A$ and $GABA_C$ receptors with higher docking score in the $GABA_A$R. Figure 6B is the docked gabazine to the $GABA_A$R binding pocket. Four putative hydrogen bonds were identified between the docked gabazine and four residues in loops A (β_2 Tyr97), B (β_2 Glu155 and β_2 Tyr157) and C (β_2 Ser201). β_2 Tyr97 is homologous to ρ_1 Phe138. Thus, this conserved Y→F mutation potentially eliminates one hydrogen bonding, making the $GABA_C$R less sensitive to gabazine. β_2 Glu155 and β_2 Tyr157 are important binding residues in the $GABA_A$R (Amin and Weiss, 1993; Newell et al., 2004). The residues corresponding to β_2 Glu155, β_2 Tyr157, and β_2 Ser201 in the ρ_1 subunit are Glu196, Tyr198, and Ser243 (or Ser242 because of an insertion of a serine). Because of identical residues at these positions in both $GABA_A$R and $GABA_C$R, they are not under our consideration. It is noteworthy that ρ_1 Y102F significantly increased the apparent affinity to gabazine. Using the structural model of $GABA_A$R as a reference, we speculate that the nature of interaction between α_1 F64 and gabazine is most likely a hydrophobic interaction. Thus, a more hydrophilic tyrosine at this position of the ρ_1 $GABA_C$R would substantially weaken this interaction. As for ρ_1 Tyr106 (α_1 Ser68), the docked gabazine in the $GABA_A$R model could not reach α_1 Ser68 in all poses. However, the docked gabazine in the $GABA_C$R binding pocket exhibited a clockwise rotation, bringing the top of the molecule to the vicinity of Tyr106 or its mutant Y106S (data not shown) while maintaining the contact with Tyr102. Thus, in the complex interacting network, ligand docking position can be altered by other available interactions. Finally, FYS240VF is not important for gabazine sensitivity, probably because phenylalanine no longer provides steric hindrance to the smaller-sized gabazine.

3-APA and 3-APMPA Sensitivity. Compared with bicuculline and gabazine, 3-APA and 3-APMPA are much smaller molecules. Our results suggest that 3-APA apparent affinity was reduced substantially by four mutations of Y102F, V140L, FYS240VF, and F138Y (Table 4). Thus, the binding site must be located in the vicinity of these four positions. Figure 6C represents a pose with 3-APA docked into an aromatic box formed by Phe138, Phe240, Tyr241, and Tyr102 [and Tyr247 and Tyr198 (behind)]. However, Val140 is not in direct contact with 3-APA. It is possible that mutation of this valine to a larger residue leucine would provide a steric hindrance to the binding and result in a decreased binding affinity for 3-APA. The amino group of the 3-APA also potentially forms a hydrogen bond with Glu196, which is homologous to β_2 Glu155 in the $GABA_A$R. With the aromatic box surrounding the docked 3-APA, it is possible that there is a π-cation interaction between 3-APA and a nearby aromatic residue(s). Thus, the binding of 3-APA to the $GABA_C$R could

be very similar to the binding of GABA to the receptor (Lummis et al., 2005). Lacking an aromatic residue in the $GABA_AR$ at the position homologous to Phe240 could reduce 3-APA affinity. 3-APMPA has structure similar to that of 3-APA. Parallel affinity reduction with these mutations for 3-APA and 3-APMPA also suggests that the structural requirements of their binding to the $GABA_CR$ are similar. Reverse mutation of the $GABA_AR$ only slightly increased 3-APA affinity suggesting other residues also make a significant contribution to the 3-APA binding.

In summary, we have identified important residues in three binding loops responsible for the $GABA_CR$ antagonist properties distinct from those of $GABA_AR$. The insights gained from this study can aid design of new antagonists for the $GABA_A$ and $GABA_C$ receptors. The approach we used in this study can also be applied to examine the mechanisms of agonist/antagonist specificity among the $GABA_AR$ subtypes.

Acknowledgments

We thank Dr. David S. Weiss from the Department of Neurobiology at the University of Alabama at Birmingham (currently in the Department of Physiology at the University of Texas at San Antonio) for kindly providing the wild type human ρ_1 and rat a_1, b_2, and γ_2 subunit constructs. We also thank Dr. Alan Gibson in the Barrow Neurological Institute for his help in proofreading the manuscript.

References

Amin J and Weiss DS (1993) $GABA_A$ receptor needs two homologous domains of the β subunit for activation by GABA, but not by pentobarbital. *Nature* **366:**565–569.
Amin J and Weiss DS (1994) Homomeric ρ_1 GABA channels: activation properties and domains. *Receptors Channels* **2:**227–236.
Amin J and Weiss DS (1996) Insights into the activation mechanism of ρ1 GABA receptors obtained by coexpression of wild type and activation-impaired subunits. *Proc Biol Sci* **263:**273–282.
Barnard EA, Skolnick P, Olsen RW, Mohler H, Sieghart W, Biggio G, Braestrup C, Bateson AN, and Langer SZ (1998) International Union of Pharmacology. XV. Subtypes of γ-aminobutyric acidA receptors: classification on the basis of subunit structure and receptor function. *Pharmacol Rev* **50:**291–313.
Böhm HJ (1994) The development of a simple empirical scoring function to estimate the binding constant for a protein-ligand complex of known three-dimensional structure. *J Comput Aided Mol Des* **8:**243–256.
Böhm HJ (1998) Prediction of binding constants of protein ligands: A fast method for the prioritization of hits obtained from the de novo design or 3D database search programs. *J Comput Aided Mol Des* **12:**309–323.
Boileau AJ, Evers AR, Davis AF, and Czajkowski C (1999) Mapping the agonist binding site of the $GABA_A$ receptor: evidence for a β-strand. *J Neurosci* **19:**4847–4854.
Boileau AJ, Newell JG, and Czajkowski C (2002) $GABA_A$ receptor β2 Tyr97 and Leu99 line the GABA-binding site: Insights into mechanisms of agonist and antagonist actions. *J Biol Chem* **277:**2931–2937.
Chang Y, Covey DF, and Weiss DS (2000) Correlation of the apparent affinities and efficacies of γ-aminobutyric acidC receptor agonists. *Mol Pharmacol* **58:**1375–1380.
Chang Y, Wang R, Barot S, and Weiss DS (1996) Stoichiometry of a recombinant $GABA_A$ receptor. *J Neurosci* **16:**5415–5424.
Cutting GR, Lu L, O'Hara BF, Kasch LM, Montrose-Rafizadeh C, Donovan DM, Shimada S, Antonarakis SE, Guggino WB, and Uhl GR (1991) Cloning of the γ-aminobutyric acid (GABA) ρ_1 cDNA: a GABA receptor subunit highly expressed in the retina. *Proc Natl Acad Sci U S A* **88:**2673–2677.
Drew CA, Johnston GA, and Weatherby RP (1984) Bicuculline-insensitive GABA receptors: studies on the binding of (−)-baclofen to rat cerebellar membranes. *Neurosci Lett* **52:**317–321.
Froestl W, Mickel SJ, Hall RG, von Sprecher G, Strub D, Baumann PA, Brugger F, Gentsch C, Jaekel J, and Olpe HR (1995) Phosphinic acid analogs of GABA. 1. New potent and selective $GABA_B$ agonists. *J Med Chem* **38:**3297–3312.
Gehlhaar D, Bouzida D and Rejto P (1999) Reduced dimensionality in ligand-protein structure prediction: covalent inhibitors of serine proteases and design of site-directed combinatorial libraries, in *Rational Drug Design: Novel Methodology and Practical Applications* (*ACS Symposium Series*) (Parrill L and Rami Reddy M eds) pp 292–311, American Chemical Society, Washington, DC.
Gehlhaar DK, Verkhivker GM, Rejto PA, Sherman CJ, Fogel DB, Fogel LJ, and Freer ST (1995) Molecular recognition of the inhibitor AG-1343 by HIV-1 protease: conformationally flexible docking by evolutionary programming. *Chem Biol* **2:**317–324.
Harrison NJ and Lummis SC (2006) Locating the carboxylate group of GABA in the homomeric rho $GABA_A$ receptor ligand-binding pocket. *J Biol Chem* **281:**24455–24461.
Holden JH and Czajkowski C (2002) Different residues in the $GABA_A$ receptor α1T60-α1K70 Region mediate GABA and SR-95531 actions. *J Biol Chem* **277:**18785–18792.
Holden J and Czajkowski C (2003) α1G124-α1L132: a novel binding site region on the $GABA_A$ receptor that undergoes distinct conformational rearrangements during ligand binding and allosteric modulation. *Soc Neurosci Abstr* **29:**50.10.
Jain AN (1996) Scoring noncovalent protein-ligand interactions: A continuous differentiable function tuned to compute binding affinities. *J Comput Aided Mol Des* **10:**427–440.
Johnston GA (1996) $GABA_C$ receptors: relatively simple transmitter-gated ion channels? *Trends Pharmacol Sci* **17:**319–323.
Krammer A, Kirchhoff PD, Jiang X, Venkatachalam CM, and Waldman M (2005) LigScore: a novel scoring function for predicting binding affinities. *J Mol Graph Model* **23:**395–407.
Lester HA, Dibas MI, Dahan DS, Leite JF, and Dougherty DA (2004) Cys-loop receptors: new twists and turns. *Trends Neurosci* **27:**329–336.
Lummis SC, L Beene D, Harrison NJ, Lester HA, and Dougherty DA (2005) A cation-π binding interaction with a tyrosine in the binding site of the $GABA_C$ Receptor. *Chem Biol* **12:**993–997.
Muegge I and Martin YC (1999) A general and fast scoring function for protein-ligand interactions: a simplified potential approach. *J Med Chem* **42:**791–804.
Murata Y, Woodward R, Miledi R, and Overman L (1996) The first selective antagonist for a $GABA_C$ receptor. *Bioorg Med Chem Lett* **6:**2073–2076.
Newell JG and Czajkowski C (2003) The $GABA_A$ receptor α1 subunit Pro^{174}–Asp^{191} segment is involved in GABA binding and channel gating. *J Biol Chem* **278:**13166–13172.
Newell JG, McDevitt RA, and Czajkowski C (2004) Mutation of glutamate 155 of the $GABA_A$ receptor β2 subunit produces a spontaneously open channel: a trigger for channel activation. *J Neurosci* **24:**11226–11235.
Ragozzino D, Woodward RM, Murata Y, Eusebi F, Overman LE, and Miledi R (1996) Design and in vitro pharmacology of a selective γ-aminobutyric acid C receptor antagonist. *Mol Pharmacol* **50:**1024–1030.
Sali A and Blundell TL (1993) Comparative protein modeling by satisfaction of spatial restraints. *J Mol Biol* **234:**779–815.
Sedelnikova A, Smith CD, Zakharkin SO, Davis D, Weiss DS, and Chang Y (2005) Mapping ρ_1 $GABA_C$ receptor agonist binding pocket: constructing a complete model. *J Biol Chem* **280:**1535–1542.
Sigel E, Baur R, Kellenberger S, and Malherbe P (1992) Point mutations affecting antagonist affinity and agonist dependent gating of $GABA_A$ receptor channels. *EMBO J* **11:**2017–2023.
Smith GB and Olsen RW (1994) Identification of a [^{3}H]muscimol photoaffinity substrate in the bovine γ-aminobutyric acidA receptor α subunit. *J Biol Chem* **269:**20380–20387.
Venkatachalam CM, Jiang X, Oldfield T, and Waldman M (2003) LigandFit: a novel method for the shape-directed rapid docking of ligands to protein active sites. *J Mol Graph Model* **21:**289–307.
Westh-Hansen SE, Rasmussen PB, Hastrup S, Nabekura J, Noguchi K, Akaike N, Witt MR, and Nielsen M (1997) Decreased agonist sensitivity of human $GABA_A$ receptors by an amino acid variant, isoleucine to valine, in the α1 subunit. *Eur J Pharmacol* **329:**253–257.
Westh-Hansen SE, Witt MR, Dekermendjian K, Liljefors T, Rasmussen PB, and Nielsen M (1999) Arginine residue 120 of the human $GABA_A$ receptor α1 subunit is essential for GABA binding and chloride ion current gating. *Neuroreport* **10:**2417–2421.
Whiting P, Wafford K and McKernan R (2000) Pharmacological subtypes of $GABA_A$ receptors based on subunit composition, in *GABA in the Nervous System: The View at Fifty Years* (Martin D and Olsen R eds) pp 113–126, Lippincott Williams & Wilkins, Philadelphia.
Zhang D, Pan ZH, Awobuluyi M, and Lipton SA (2001) Structure and function of $GABA_C$ receptors: a comparison of native versus recombinant receptors. *Trends Pharmacol Sci* **22:**121–132.

Address correspondence to: Dr. Yongchang Chang, Division of Neurobiology, Barrow Neurological Institute, 350 West Thomas Road, Phoenix, AZ 85013. E-mail: yongchang.chang@chw.edu